

Electronic band structure of rare-earth ferroelastics: theoretical investigations

SEVKET SIMSEK^{a*}, GOKAY UGUR^b, SULE UGUR^b, AMIRULLAH M. MAMEDOV^{c,d}, EKMELE OZBAY^c

^aDepartment of Material Science and Engineering, Faculty of Engineering, Hakkari University 30000, Hakkari, Turkey

^bDepartment of Physics, Faculty of Sciences, Gazi University, 06500, Ankara, Turkey

^cNanotechnology Research Center (NANOTAM), Bilkent University, 06800 Bilkent, Ankara, Turkey

^dInternational Scientific Center, Baku State University, Baku, Azerbaijan

In the present work, the electronic band structure and optical properties of $\text{RE}_2(\text{MoO}_4)_3$ are investigated. The ground state energies and electronic structures were calculated using density functional theory (DFT) within the generalized-gradient approximation (GGA). The real and imaginary parts of dielectric functions and hence the optical functions such as energy-loss function, the effective number of valence electrons and the effective optical dielectric constant were also calculated. The main structure element in all our compounds is the MoO_4 tetrahedron. The presence of the MoO_4 tetrahedra in the lattice of $\text{Gd}_2(\text{MoO}_4)_3$, the similarity of the band structure and optical spectra of $\text{Gd}_2(\text{MoO}_4)_3$ to those other tetraoxoanions of molybdenum demonstrate an important role of the MoO_4 tetrahedra in the formation of the energy spectrum of $\text{Gd}_2(\text{MoO}_4)_3$ and other $\text{RE}_2(\text{MoO}_4)_3$ compounds. This means that the MoO_4 tetrahedra determine the lower edge of the conduction band and the upper edge of the valence band, and the conduction band is split into two subbands. The optical properties of $\text{RE}_2(\text{MoO}_4)_3$ are in good agreement with this conclusion and previous experimental data.

(Received January 16, 2017; accepted February 12, 2018)

Keywords: ab initio calculation, Rare-Earth Ferroelastics, Electronic structure, Optical properties

1. Introduction

During the past few decades, much attention has been paid to rare-earth oxides for developing novel optical devices such as lasers, fiber amplifiers, displays and sensors [1]. Also, rare earth doped single crystals $\text{RE}_2(\text{MoO}_4)_3$ have been extensively studied as a candidate material for applications such as fluorescence [2], phosphors, ionic conductors [3], magneto-electric switching [4], second harmonic generation [5], white light emitting diodes [6]. One of the most important group among these compounds is the family of acentric rare-earth ($\text{RE}=\text{Gd}, \text{Dy}, \text{Tb}, \text{Eu}$ and Sm) molybdates that are oxygen-tetrahedral ferroelectrics-ferroelastics – $\text{RE}_2(\text{MoO}_4)_3$. $\text{RE}_2(\text{MoO}_4)_3$ show different structural types depending on the temperature [7-8]. The presence in $\text{RE}_2(\text{MoO}_4)_3$ of three independent groups of MoO_4 tetrahedra with different Mo-O bonds and the relative displacements of RE^{3+} ions and the MoO_4 sublattices (Mo^{6+} ion coordinates by four oxygen ions, and the resulting molybdenum coordination polyhedra can be strongly distorted), as a result of a phase transition alter many macroscopic and microscopic parameters of these compounds [8]. The question of the nature of the ferroelectric state of these oxides is closely related to the electron interactions in them. It would be interesting to study the electron structure and nature of chemical bonds in $\text{RE}_2(\text{MoO}_4)_3$, as well as the role of the MoO_4 tetrahedra in the formation of the energy spectrum of electrons.

In the present work, the electronic band structure and optical properties of $\text{RE}_2(\text{MoO}_4)_3$ are investigated. The

ground state energies and electronic structures were calculated using the density functional theory (DFT) within the generalized-gradient approximation (GGA) [9]. The real and imaginary parts of dielectric functions and hence the optical functions such as energy-loss function, the effective number of valence electrons and the effective optical dielectric constant were also calculated. The main structure element in all of our compounds is the MoO_4 tetrahedron. The presence of the MoO_4 tetrahedra in the lattice of $\text{Gd}_2(\text{MoO}_4)_3$, the similarity of the band structure and optical spectra of $\text{Gd}_2(\text{MoO}_4)_3$ to those other tetraoxoanions of molybdenum demonstrate an important role of the MoO_4 tetrahedra in the formation of the energy spectrum of $\text{Gd}_2(\text{MoO}_4)_3$ and other $\text{RE}_2(\text{MoO}_4)_3$ compounds. This means that the MoO_4 tetrahedra determine the lower edge of the conduction band and the upper edge of the valence band, and the conduction band is split into two subbands. The optical properties of $\text{RE}_2(\text{MoO}_4)_3$ are in good agreement with this conclusion and previous experimental data [10].

2. Method of calculation

In the present paper, all calculations have been carried out using the ab-initio total-energy and molecular-dynamics program VASP (Vienna ab-initio simulation program) developed at the Faculty of Physics of the University of Vienna [11-14] within the density functional theory (DFT) [15]. The exchange-correlation energy function is treated within the GGA (generalized gradient

approximation) by the density functional of Perdew et al. [9]. We get good convergence using a $6 \times 6 \times 3$ Monkhorst-Pack [16] mesh grid for the total-energy calculation with a cut off energy of 532 eV for $Gd_2(MoO_4)_3$ compound. The electronic iterations convergence is 1.0×10^{-5} eV using the Normal (blocked Davidson) algorithm and reciprocal space projection operators. The ion-electron interactions were modeled by the optimized norm-conserving pseudopotentials [17] for all constituent elements, and the O $2s^2 2p^4$, Mo $4d^5 5s^1$, RE (n=6 (Sm), n=7 (Gd, Eu), n=10 (Dy), n=9 (Tb)) [Xe] $4f^n 6s^2$ electrons were treated as the valence electrons, respectively[1]. It is well known that standart GGA approaches have a major deficiency for studying systems containing transition metal or rare-earth metal ions with partially filled d (or f) shells. Thus, the GGA+U[18] method in which the Hubbard U is applied on RE (6.0 eV) and Mo (3.0 eV on d-orbitals), was employed to perform the electronic structure calculations on $RE_2(MoO_4)_3$. Based on the calculated electronic band structure, the optical properties for $RE_2(MoO_4)_3$ were determined, and the dispersion of linear response of optical susceptibility was predicted.

3. Results and discussion

3.1 Electronic properties

We have studied $Gd_2(MoO_4)_3$ compound in the monoclinic phase with space groups $P2/c$. The electronic band structure of $Gd_2(MoO_4)_3$ - GMO along the high symmetry directions have been calculated by using the equilibrium lattice constants and is given in Fig .1.

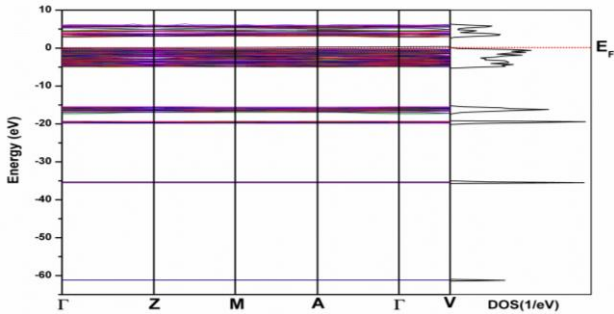


Fig. 1. The calculated electronic band structure and Density of the State for $Gd_2(MoO_4)_3$.

First principle calculations can identify the electronic structure and chemical bonding through the investigations of density of states (DOS) and band structure. The band gap calculated here is 3.026 eV. The valence band (VB) maximum and the conduction band (CB) minimum are both locate at Γ point, so GMO is a direct insulator.

In the same Fig. DOS is shown. We can see that the semicore orbitals of Mo are highly localized, which show as a peak in the DOS (-35 eV). The lower VB located at approx. -15 to -20 eV are predominantly composed of O 2s states, slightly hybridized with Gd 5p states. The upper VB are mainly composed of O 2p states, slightly hybridized with Mo 5d states, yielding a band width of about 5.0 eV.

The CB of GMO mainly consists of unoccupied orbitals of cations. The lowest CB, with width of approx. 3.0 eV, mainly consists of Mo 5d states, with hybridized with O 2p states. For the tetrahedron crystal effect, the Mo 5d states are split into two parts (“e” state that contains 3 $d_{x^2-y^2}$ and 3 d_z^2 states, and “ t_2 ” state that contains 3 d_{xy} , 3 d_{yz} , 3 d_{xz} states), which shows two distinct parts below and above 4 eV. The conduction bands above 8 eV mainly exhibit the characteristics of Gd 6f-states. From DOS results, we also can say that Mo – O bonds show more covalent characteristic than Gd –O bonds. There are two kinds of Gd –O bonds in a $Gd_2(MoO_4)_3$ structure where GdO_7 polyhedron is slightly distorted [10].

3.2. Optical Properties

At the level of a linear response, the polarization can be calculated using the following relation [19]:

$$P^i(\omega) = \chi_{ij}^{(1)}(-\omega, \omega) E^j(\omega) \quad (1)$$

Where $\chi_{ij}^{(1)}$ is the linear optical susceptibility tensor [20]. The dielectric function $\epsilon_{ij}(\omega) = 1 + 4\pi\chi_{ij}^{(1)}(-\omega, \omega)$ and the imaginary part of $\epsilon_{ij}(\omega)$, $\epsilon_2^{ij}(\omega)$ is given b

$$\epsilon_2^{ij}(\omega) = \frac{e^2}{\hbar\pi} \sum_{nm} \int d\vec{k} f_{nm}(\vec{k}) \frac{v_{nm}^i(\vec{k}) v_{nm}^j(\vec{k})}{\omega_{nm}^2} \delta(\omega - \omega_{nm}(\vec{k})) \quad (2)$$

where n, m denote energy bands, $f_{nm}(\vec{k}) \equiv f_n(\vec{k}) - f_m(\vec{k})$ is the Fermi occupation factor. The real part of $\epsilon_{ij}(\omega)$, $\epsilon_1^{ij}(\omega)$, can be obtained by using the Kramers-Kronig transformation [20]. Because the Kohn-Sham equations determine the ground state properties, the unoccupied conduction bands as calculated, have no physical significance.

The corresponding energy-loss functions, $L(\omega)$, were calculated using eq.(3) and are also presented in Fig. 5. The $L(\omega)$ describes the energy loss of fast electrons traversing the material. The sharp maxima in the energy loss function are associated with the existence of plasma oscillations [19-20].

$$L(\omega) = \frac{\epsilon_2(\omega)}{\epsilon_1^2(\omega) + \epsilon_2^2(\omega)} \quad (3)$$

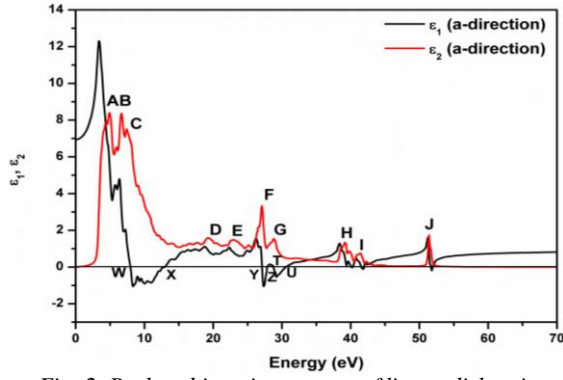


Fig. 2. Real and imaginary parts of linear dielectric function along a-direction for $Gd_2(MoO_4)_3$

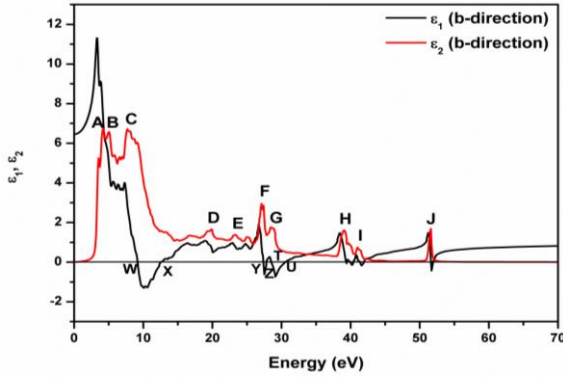


Fig. 3. Real and imaginary parts of linear dielectric function along b-direction for $Gd_2(MoO_4)_3$

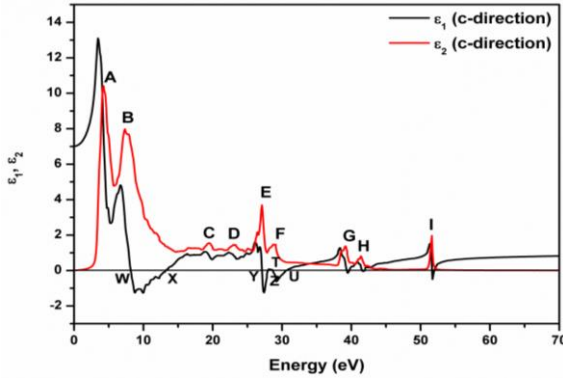


Fig. 4. Real and imaginary parts of linear dielectric function along c-direction for $Gd_2(MoO_4)_3$.

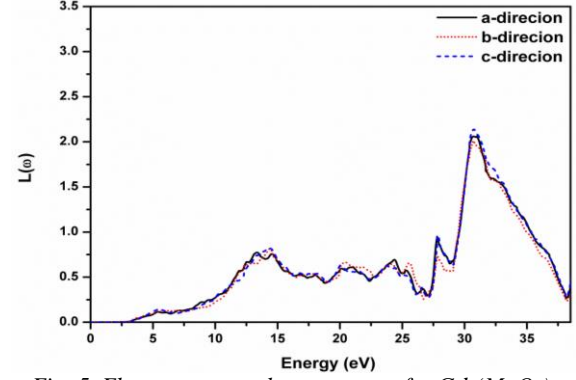


Fig. 5. Electron energy-loss spectrum for $Gd_2(MoO_4)_3$.

We first calculated the real and imaginary parts of linear dielectric function of $Gd_2(MoO_4)_3$ – GMO along main crystallographic directions (Fig. 2-4). In order to calculate the optical response by using the calculated band structure, we have chosen a photon energy range of 0-70 eV and have seen that a 0-50 eV photon energy is sufficient for most optical functions. It is clear from these figures that the spectra of ϵ_{ij} of GMO have a structure concentrated in two wide bands at $E=3.0$ -14.0 eV (Table 1). The main structure element in all $RE_2(MoO_4)_3$ is the MoO_4 tetrahedron. The presence of the MoO_4 tetrahedra in the lattice of GMO, the similarity of the ϵ_{ij} of GMO to those of the other tetraoxyanions of Mo demonstrate an important role of the MoO_4 tetrahedra in the formation of the energy spectrum of GMO and other $RE_2(MoO_4)_3$. This means that the MoO_4 tetrahedra determine the lower edge of the conduction band and the upper edge of the valence band, and the conduction band is split into two sub-bands separated by 2.4 eV. Such splitting is typical of the electron states of the d-transition metals subjected to a crystal field.

Table 1. Energy positions (eV) of principal singularities of optical responses for oxygen-tetrahedral-ferroelectrics at photon energies 3.0-17.0 eV.

maximum peak values of ϵ_2 (eV), our calculations - GMO			T=300 K, experimental data[5]				
a-direction	b-direction	c-direction	GMO	DMO	TMO	EMO	SMO
			3.16	-	-	-	-
			3.62	3.68	3.45	3.35	3.70
			4.07	-	-	-	-
			4.30	-	-	-	-
4.86	4.14	4.32	5.20	4.54	4.40	4.37	4.60
			5.65	-	-	-	-
			6.00	5.29	5.52	5.30	5.52
6.67	5.41	7.38	6.45	-	-	-	-
			-	-	7.13	6.70	6.67
			7.01	7.59	7.82	-	7.36

maximum peak values of ε_2 (eV), our calculations - GMO			T=15 K	T=300 K, experimental data[5]				
a-direction	b-direction	c-direction	GMO	GMO	DMO	TMO	EMO	SMO
7.56	7.74	9.63	7.41	-	-	-	-	-
			-	8.54	8.30	8.20	8.30	8.40
19.44	19.99	28.88	19.68	19.70	20.36	-	-	20.00
			-	-	-	-	-	-
23.23	23.23	27.19	23.07	23.75	-	23.75	23.07	23.90
			24.43	-	-	-	-	-
27.02	27.19	28.99	-	26.47	27.45	-	26.70	26.70
			26.70	-	-	-	-	-
28.82	28.99	39.25	30.31	31.90	29.41	28.28	29.85	-

Table 2. The energy values at the zero point of real part of dielectric function for $Gd_2(MoO_4)_3$.

	W	X	Y	Z	T	U
a-direction	7.92	12.608	27.189	27.731	28.99	30.62
b-direction	9.0	12.608	27.73	28.64	28.82	30.804
c-direction	8.1	13.33	27.19	27.73	28.82	30.804

An increase in the energy of the incident photons results in a rapid fall of the ε_{ij} and there is no clear structure in the spectra of ε_{ij} at energies above 35.0 eV (Table 1) The absence of singularities in the spectra of ε_{ij} of GMO, at photon energies above 35.0 eV shows that the valence and conduction bands are separated by large gaps from the other deep-level energy bands or that transitions from semicore levels to the conduction band are forbidden by the selection rules.

The GMO studied so far have ε_1 are equal to zero in the energy region between 8.0 eV and 30 eV for decreasing and increasing of ε_1 (Table 2). In addition, values of ε_1 versus photon energy have main peaks in the energy region 3.0-55.0 eV. Some of the principal features and singularities of the ε_{ij} for GMO is shown in Table 2. The peaks of the ε_{ij} correspond to the optical transitions from the valence band to the conduction band are in agreement with the previous results [10].

The corresponding energy loss functions, $L(\omega)$, were calculated using eq. (6) and also presented in Fig.2-4. The $L(\omega)$ describes the energy loss of fast electron traversing the material. The sharp maxima in the $L(\omega)$ are associated with the existence of plasma oscillations [19]. The curve of $L(\omega)$ has a maximum near 30 eV for GMO.

4. Conclusion

In the present work, we conducted a detailed investigation of the electronic, and frequency-dependent linear optical properties of the $Gd_2(MoO_4)_3$ crystal using the density functional methods. The result of the structural optimization implemented using the GGA are in good agreement with the experimental results. We have examined photon-energy dependent dielectric functions, some optical properties such as the energy-loss function for $Gd_2(MoO_4)_3$.

Acknowledgements

This work is supported by the projects DPT-HAMIT, DPT-FOTON, and NATO-SET-193 and TUBITAK under project nos., 113E331, 109A015, and 109E301. One of the authors (Ekmel Ozbay) also acknowledges partial support from the Turkish Academy of Sciences.

References

- [1] G. Adachi, N. Imanaka, Z. C. Kang, Binary Rare Earth Oxides, Springer Netherlands, 2005.
- [2] H. Hao, H. Lu, R. Meng, Z. Nie, G. Ao, Y. Song, Y. Wang, X. Zhang, Journal of Alloys and Compounds. **695**, 2065 (2017).
- [3] Y. Wang, X. Liu, P. Niu, L. Jing, W. Zhao, Journal of Luminescence **184**, 1 (2017).
- [4] L. Bufaiçal, G. Barros, L. Holanda, I. Guedes, Journal of Magnetism and Magnetic Materials **378**, 50 (2015).
- [5] M. Li, S. Sun, L. Zhang, Y. Huang, F. Yuan, Z. Lin, Optics Communications **355**, 89 (2015).
- [6] V. V. Sinitsyn, B. S. Redkin, A. P. Kiselev, S. Z. Shmurak, N. N. Kolesnikov, V. V. Kveder, E. G. Ponyatovsky, Solid State Sciences **46**, 80 (2015).
- [7] T. F. Connolly, Ferroelectric Materials and Ferroelectricity, Springer, 2013.
- [8] M. E. Lines, A. M. Glass, Principles and Applications of Ferroelectrics and Related Materials. New York, Oxford University Press, 1977.
- [9] J. P. Perdew, S. Burke, M. Ernzerhof, Phys Rev Lett. **77**, 3865 (1996).
- [10] A. M. Mamedov, Sov. Phys. JETP (English Transl.) **63**, 305 (1986).
- [11] G. Kresse, J. Hafner, Phys Rev B **47**, 558 (1993).

-
- [12] G. Kresse, J. Furthmüller, *Comput Mater Sci.* **6**, 15 (1996).
- [13] G. Kresse, D. Joubert, *Phys Rev B.* **59**, 1758 (1999).
- [14] G. Kresse, J. Furthmüller, *Phys Rev B.* **54**, 11169 (1996).
- [15] P. Hohenberg, W. Kohn, *Phys. Rev.* **136**, B864 (1964).
- [16] H. J. Monkhorst, J. D. Pack, *Phys. Rev. B* **13**, 5188 (1976).
- [17] Z. H. Levine, D. C. Allan, *Phys. Rev. Lett.* **63**, 1719 (1989).
- [18] B. Himmetoglu, A. Floris, S. Gironcoli, M. Cococcioni, *Int. J. Quantum Chem.* **114**, 14 (2014).
- [19] H. R. Philipp, H. Ehrenreich, *Phys. Rev.* **129**, 1550 (1963).
- [20] M. Dressel, G. Grüner, *Electrodynamics of Solids: Optical properties of Electrons in Matter.* Cambridge, Cambridge University Press, (2003).

*Corresponding author: ssimsek_001@hotmail.com